Energy 171 (2019) 624–630

Contents lists available at ScienceDirect

Energy

journal homepage: www.elsevier.com/locate/energy

Numerical and experimental investigation on configuration optimization of the large-size ionic wind pump

Jianfei Zhang*, Lingjian Kong, Jingguo Qu, Shuang Wang, Zhiguo Qu

Key Laboratory of Thermo-Fluid Science and Engineering, Ministry of Education, School of Energy and Power Engineering, Xi'an Jiaotong University, Xi'an, 710049, China

ARTICLE INFO

Article history:
Received 29 September 2018
Received in revised form
24 December 2018
Accepted 15 January 2019
Available online 16 January 2019

Keywords:
Ionic wind pump
Large-size
Configuration optimization
Numerical simulation
Experiment

ABSTRACT

An ionic wind pump is an energy-saving device that can produce a volume flow when electrodes are applied with high voltage. Compared to the traditional methods, ionic wind pumps possess the advantages of low energy consumption, no moving parts, compact structure and flexible design. In this study, a large-size ionic wind pump, consisting of many single regular hexagonal needle-ring ionic wind generators, was developed as the preliminary model. However, its experimental performance was not as good as our expectations. In order to improve this preliminary model, a simulation method was used to investigate the configuration factors of the single ionic wind pump. In the optimized model, mesh gap is 6 mm, eccentricity is 0.26, section area is 238.44 mm^2 and needle electrode number is 3. In subsequent experiments, the final optimized large-size ionic wind pump showed a great promotion in velocity, and the maximum average velocity of the optimized pump was higher than the preliminary model by 13.3%. Our numerical simulation and experiment results have practical significance in designing ionic wind pumps.

1. Introduction

Mechanical fans or pumps are widely used to drive air flow in electronic devices, air conditioners and air purifiers. However, with the rapid development of science and technology, mechanical fans or pumps could not meet the demands for low acoustic, low energy consumption and low risk of damage on moving parts. As a novel compact cooling device, the ionic wind pump does not have moving parts and could noiselessly work in a much lower power compared to conventional cooling devices [1–4]. Therefore, the ionic wind pump has great potential to meet severe demands currently and even more severe demands in the future.

An ionic wind pump is an application of ionic wind induced by a corona discharge phenomenon [5,6]. As shown in the Fig. 1, the corona discharge is generated when a large electric potential is applied between two electrodes [7]. The gas ions are accelerated and exchange momentum in the electric field, generating a drag of the bulk fluid, which is referred to as ionic wind. The great application prospects of ionic wind pumps in enhancing heat transfer and driving air flow attract a lot of researchers around the world [8–11]. Both numerical and experimental investigations of ionic wind pumps have been carried out in recent years. Kim [12] conducted a series of experiments to investigate velocity and energy conversion efficiency of ionic wind pumps in a multistage configuration. The experimental results reveal the relation between the number of stages, current, voltage, velocity and energy conversion efficiency. S. Ohyama [13] presented an experimental method to investigate the dependency between ionic wind velocity, current and frequency of applied AC voltage. QIU [14] designed a needle-mesh type electrohydrodynamic (EHD) gas pump and placed several single-stage pumps in a series to enhance velocity and energy conversion efficiency. When the number of the stage is 25, the outlet velocity can achieve 16.1 m/s and volumetric flow can achieve 303.5 L/min. Li [15] measured the ionic wind velocity and current with respect to electrode geometries and distance between electrodes and voltages. Furthermore, an empirical model is suggested based on the experimental data, which can be used to design ionic wind pumps. Lee [16] reported a novel ionic wind pump with parallel integration in which numerous single ionic wind pumps with a needle-cylinder configuration are tightly integrated. The experimental results demonstrated that the velocity can achieve a maximum value of 2.2 m/s when the voltage is 10.5 kV. The application of printed circuit boards (PCBs) showed advantages in the

* Corresponding author.
E-mail address: zhangjf@xjtu.edu.cn (J. Zhang).

https://doi.org/10.1016/j.energy.2019.01.086
0360-5442/

Nomenclature

a	eccentricity
d_1	the distance between the needle electrode and the side of hexagon m
d_2	the side length of regular hexagon m
V	electric potential V
q	space charge density $C \cdot m^{-3}$
P	pressure Pa
$\boldsymbol{F}$	Coulomb force N
$\boldsymbol{J}$	current density $A \cdot m^{-1}$
$\boldsymbol{E}$	electric field strength $V \cdot m^{-1}$
$\boldsymbol{U}$	velocity $m \cdot s^{-1}$

Greek letters

ε	dielectric permittivity $F \cdot m^{-1}$
μ_E	ion mobility $m^2 \cdot V^{-1} \cdot s^{-1}$
ρ	gas density $kg \cdot m^{-3}$
ν	kinematic viscosity $m^2 \cdot s^{-1}$

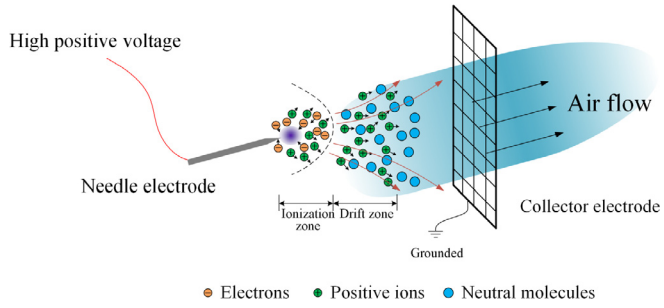

Fig. 1. The generation process of ionic wind.

fabrication of ionic wind pumps and stacking the multiple layers in series, which could greatly increase the volumetric flow. Besides the experimental investigation, some numerical simulation investigations are carried out to investigate ionic wind pumps. M Rickard and D Dunn-Rankin [17] numerically investigated an ion-driven wind generator using FEMLAB, a commercial multi-physics solver. The simulation results agreed well with the experimental results. In the simulation, the velocity at the tube core is much higher than in the outer regions and the generator could offer a better performance when the angle between needle tip and ring leading edge was 45°. Pérez [18] studied a two-dimensional EHD flow occurring between a blade and a plate electrode. The simulations, which are based on direct simulation without any turbulent model, were conducted to analyze the evolution of velocity profiles and flow patterns with a numerical approach. Lin Zhao and Kazimierz Adamiak [19] numerically investigated the effect of EHD in a pin-plate system in compressed air using FLUENT software. In the numerical algorithm, the boundary-element method and the finite-element method were applied. The simulation results revealed the characteristics of EHD flow on corona discharge under different gas pressure.

Although many researchers have devoted themselves to the study of ionic wind pumps, investigations about the large-size ionic wind pumps and numerical simulation of a three-dimensional model are not enough. In this paper, a study on a large-size ionic wind pump is carried out. First, an ionic wind pump, which consists of many single regular hexagonal needle-ring ionic wind pumps, is designed as a preliminary model. The experimental results demonstrate that the outlet velocity is lower than our expectation and the uniformity of outlet velocity is not good enough. Based on this preliminary model, a new large-size ionic wind pump is developed. In this new pump, the needles are placed in the hexagonal rings, instead of being placed in the intersectional points of the rings, and the ring electrodes are replaced by the mesh electrodes. Particular attention is devoted to enhancing velocity of ionic wind pumps. Considering the low calculation efficiency of the numerical simulation of a large-size integrated configuration, the single regular hexagonal ionic wind pump unit is regarded as the study object to carry out the numerical investigation. In order to figure out the effect of configuration on velocity, optimization work is carried out with 3D models in COMSOL Multiphysics. Needle number, eccentricity of needle electrodes, size of regular hexagon and mesh gap are regarded as adjustable factors to investigate their influences. After finishing investigations about the configuration factors of single ionic wind pump, a large-size ionic wind pump is fabricated using the configuration optimization result. In subsequent verification experiments, the velocity characteristics of the optimized pump show great improvement.

2. Numerical and experimental study on preliminary design

2.1. Preliminary design of an ionic wind pump

At first, a large-size ionic wind pump is designed as the preliminary model. Fig. 2 shows the 3-D configuration of this preliminary model. In this configuration, needle electrodes, pointing at the centers of the regular hexagonal collector electrodes, are placed in the junctions of the regular hexagonal ring electrodes. The shape of the integrated ionic wind pump is a rectangle (250 mm × 74 mm). The diameter and length of the needle electrode are 1 mm and 6 mm, respectively. The side length of the regular hexagon is 9.58 mm and the distance between corona electrode and collector electrode is 16 mm.

2.2. Experiment rig

Figs. 3 and 4 show the schematic diagram and photography picture the experimental test unit. The ionic wind pump is composed of two separated electrode boards: a corona electrode board and a collector electrode board. Both of the boards consist of many regular hexagonal rings. Needles in the corona electrode board are applied with a negative high voltage while the collector electrode board is set to be grounded. The high-voltage DC power supply (TRC2020N20-300) is used to apply a high electric potential between the two electrode boards, and its uncertainty is 0.1%. The corona electrode board is applied with a negative high voltage and the collector electrode board is grounded. The voltage and total current are obtained from the display of the power supply. A rotating anemometer (Victor 816B) is placed 10 mm away from the outlet to measure the wind speed, and its uncertainty is 0.32%.

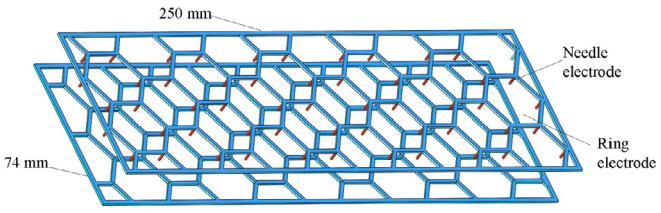

Fig. 2. The 3-D schematic diagram of the preliminary model.

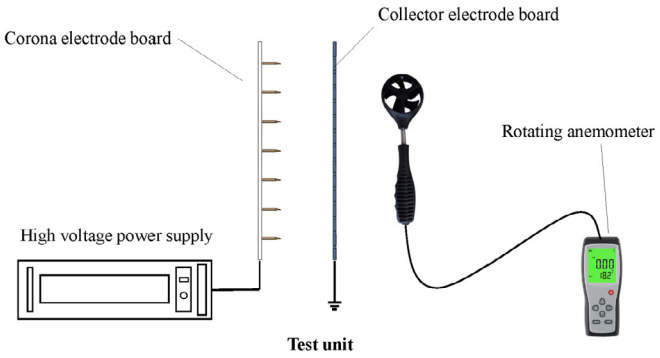

Fig. 3. The schematic diagram of the experimental test unit.

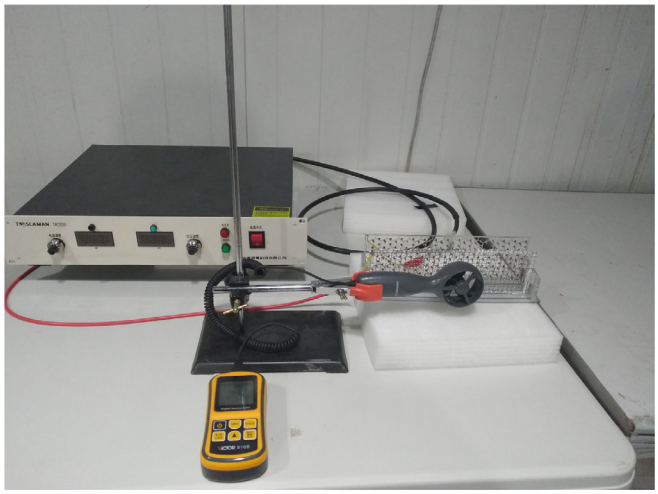

Fig. 4. The photography picture of experimental test unit.

During the experiment, the environment temperature is maintained at 20 °C.

2.3. Physical model and numerical solution method

2.3.1. Physical model and boundary conditions

Fig. 5 shows the physical model of preliminary model, and the computational domain is *abcd* in the figure. Air enters the ionic wind pump from the inlet, ionic wind is generated between corona electrodes and collector electrodes and flows out from the outlet. Electric field and flow field are calculated in the computational domain. In the numerical simulation, air is considered as dry air, and the influence of humidity is ignored. Fig. 6 shows the grid diagram in COMSOL Multiphysics. The quality of grid is able to guarantee the calculation precision to get reliable results in numerical simulation. The boundary conditions of numerical simulation in COMSOL Multiphysics are shown in Table 1.

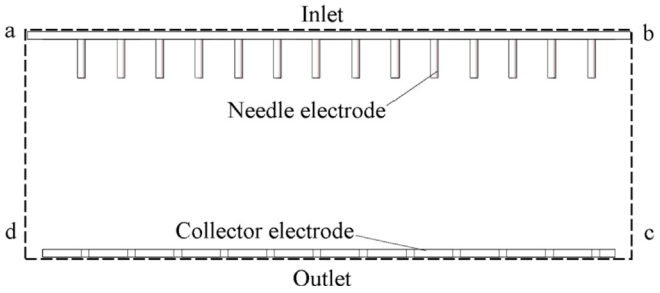

Fig. 5. The cross-sectional figure of the physical model.

2.3.2. Governing equations

Ionic wind is a complicated physical phenomenon, and its production is an interaction of many physical fields. The electrical discharge in the interelectrode space of an ionic wind pump is described by Poisson's equation:

$$\nabla \bullet E = -\nabla^2 V = \frac{q}{\varepsilon}, \tag{1}$$

where $\boldsymbol{E}$ is the electric field strength, V is the electric potential, q is the space charge density and ε is the dielectric permittivity. The current density $\boldsymbol{J}$ of the electric current generated by charge drifting is defined as:

$$J = \mu_E E q, \tag{2}$$

where μ_E is the ion mobility.

Under the assumption that the fluid is an incompressible Newtonian fluid, the flow can be described by the Navier-Stokes equation:

$$\nabla \bullet (\rho \boldsymbol{UU}) = -\nabla P + \nu \nabla^2 \boldsymbol{U} + \boldsymbol{F}, \tag{3}$$

where ρ is the gas density, $\boldsymbol{U}$ is the velocity, ν is the kinematic viscosity, P is the pressure and $\boldsymbol{F}$ is the Coulomb force.

2.3.3. Solution method and validation of simulation results

The simulation method is based on COMSOL Multiphysics, a commercial package which could carry out 3-D numerical simulations. In COMSOL Multiphysics, a high positive DC voltage is applied to the needle electrodes, and the voltage of collector electrode is set as 0 V. For calculating charge density distribution, a space charge density q_0 is applied to the surface of the needle electrodes. In order to get q_0, the Katpzov hypothesis is adopted, which suggests that the charge density will remain unchanged after the corona is initiated. In the calculation of flow field, the no-slip boundary condition is applied to the surface of needle electrodes and collector electrodes to calculate the velocity characteristics of the air flow.

In order to check the reliability of the simulation method, the outlet average velocity results measured from the experiments are used in comparison with the simulation results. As is shown in Fig. 7, simulation results tally well with experimental results. In the range of voltage from 10 kV to 14 kV, maximum error is only 6.2% when the voltage is 10 kV. Therefore, the simulation method which we adopt could be thought of as a reliable method.

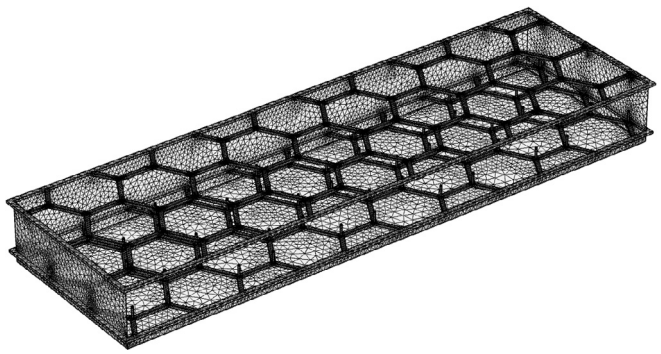

Fig. 6. The grid diagram in COMSOL Multiphysics.

Table 1
Boundary conditions.

Surface	Electrostatic field	Space charge field	Velocity field
Corona electrode	$V=V_0$	$\rho=\rho_0$	No slip
Collector electrode	$V=0$	Zero flux	No slip
Inlet	Zero charge	Zero flux	Pressure = 1 atm
Outlet	Zero charge	Zero flux	Pressure = 1 atm
Others	Zero charge	Zero flux	No slip

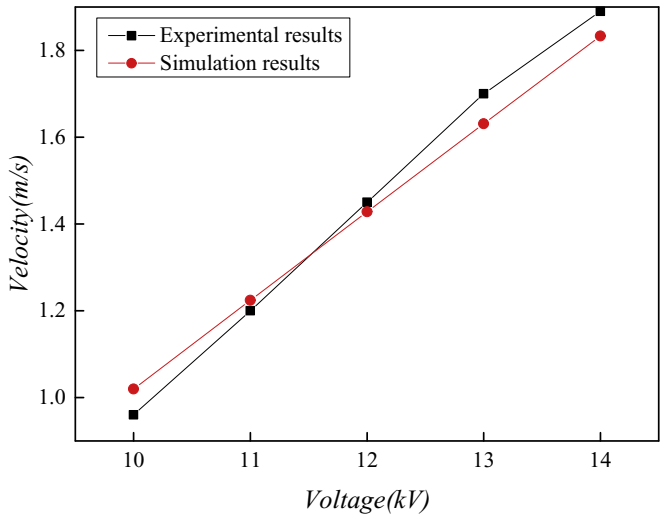

Fig. 7. Verification of the simulation method.

2.4. Flow characteristics of preliminary design of ionic wind pump

Fig. 8 shows the velocity distribution of the preliminary model when applied voltage is 14 kV. As is shown in this figure, the preliminary model does not perform well in the uniformity of outlet velocity. The simulation results show that the average and maximum of outlet velocity are 1.83 m/s and 3.47 m/s, respectively. Compared to our expectation, the outlet velocity is lower and the difference between average and maximum is a little bigger. Thus, more work is required in enhancing outlet velocity and improving the uniformity of outlet velocity distribution.

3. Numerical parametric studies on improvement design of ionic wind pump

Considering that the large-size ionic wind pump consists of repeated units, a single unit is regarded as the study subject to increase the calculation efficiency. In the improvement design, the ring electrode is replaced by the mesh electrode to enhance the

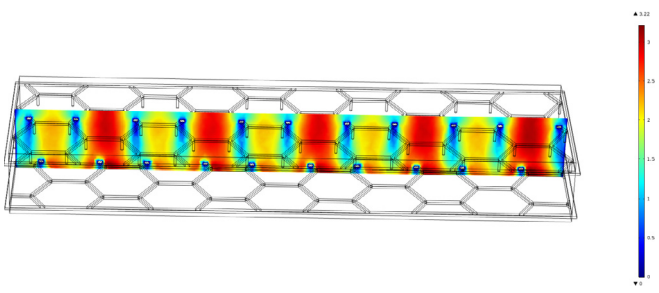

Fig. 8. Velocity characteristics of the preliminary model.

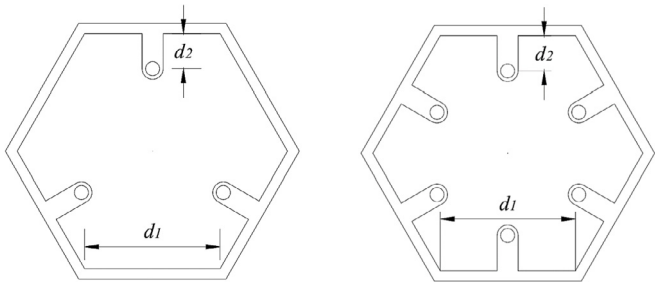

Fig. 9. The distribution of the needle electrodes.

density of the collector electrode. The distribution of needle electrodes is improved to increase needle electrode number so that more air jets will be produced. In order to further optimize the pump, the configuration factors are investigated from the eccentricity, mesh gap, the section area of regular hexagon and needle electrode number.

Fig. 9 shows the distribution of needle electrodes when needle electrode number is 3 and 6. In this diagram, $d1$ represents the distance between the needle electrode and the side of hexagon, and $d2$ represents the side length of regular hexagon. Eccentricity a ($a = d2/d1$) is regarded as a factor to investigate the influence of the location of needle electrodes. Fig. 10 shows the configuration of mesh electrode and the mesh gap is defined as the distance between metal wires.

3.1. Effect of the eccentricity of needle electrodes

The eccentricity of needle electrodes is an important factor that determines the distribution of needle electrodes and affects the velocity characteristics directly. In the investigation of eccentricity, the applied voltage is 14 kV, the number of needle electrodes is 3, mesh gap is 5 mm and the side length of regular hexagon is 9.58 mm.

Fig. 11 shows the effect of eccentricity on average velocity and maximum velocity on outlet section. As is shown in this figure, the average velocity achieves maximal value, which is 2.47 m/s, when the eccentricity is 0.26. The maximum velocity achieves maximal value, which is 3.93 m/s, when the eccentricity is 0.43. It can be found that when the eccentricity is close to 0 or 1, indicating that the needle electrodes are close to the sides or the center of hexagon,

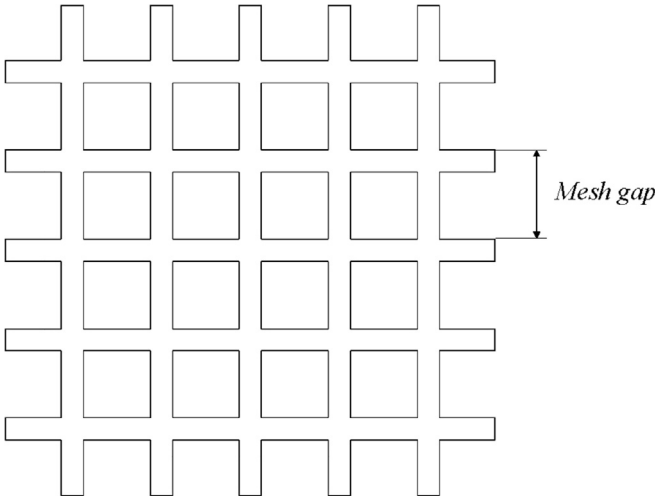

Fig. 10. The schematic diagram of the mesh electrode.

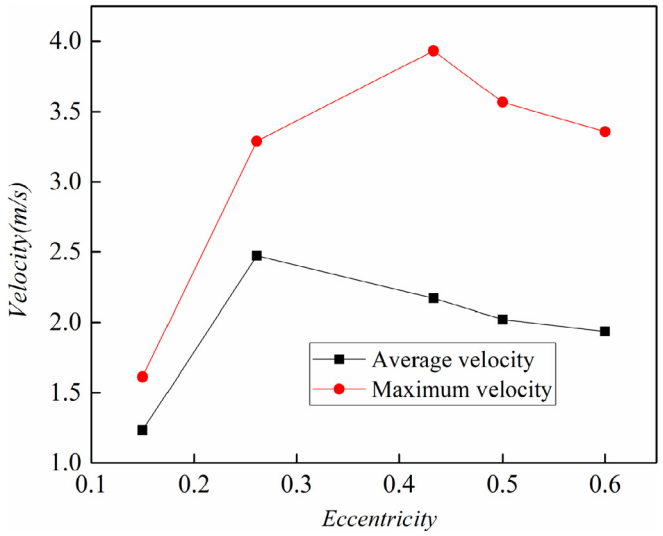

Fig. 11. The velocity characteristics with the eccentricity of 0.15, 0.26, 0.43, 0.5, 0.6, respectively.

both average velocity and maximum velocity will decline. The reason could be that both the sides of hexagon and the interaction between needle electrodes have adverse effects on the increase of velocity. Considering the velocity characteristics, 0.26 could be regarded as the optimum value of eccentricity.

3.2. Effect of mesh gap

Mesh gap is an important factor that could significantly influence the outlet velocity of the ionic wind pump. In the investigation of mesh gap, we build a series of models with one needle electrode and the applied voltage, eccentricity and side length of regular hexagon are 14 kV, 0.26 and 6.2 mm, respectively.

Fig. 12 shows the effect of mesh gap on average velocity and maximum velocity on outlet section. As is shown in this figure, average velocity and maximum velocity increase with the increase of mesh gap and slowly decline after maximum value. The maximum value of average velocity is 2.74 m/s when the mesh gap is 6 mm, and the maximum value of maximum velocity is 5.03 m/s when the mesh gap is 4 mm. When the mesh gap is 3 mm, both average velocity and maximum velocity are low. It could be concluded that the velocity will be significantly harmed by the huge flow resistance of mesh electrode if the gap of mesh electrode is too small. On the other hand, when the mesh gap is 7 mm, velocity also will decline because the effective area of mesh electrode is not large enough in this situation. Thus, a proper mesh gap could efficiently enhance the average velocity on outlet section. Considering the outstanding performance in velocity characteristics, 6 mm could be regarded as the optimum value of mesh gap in this investigation.

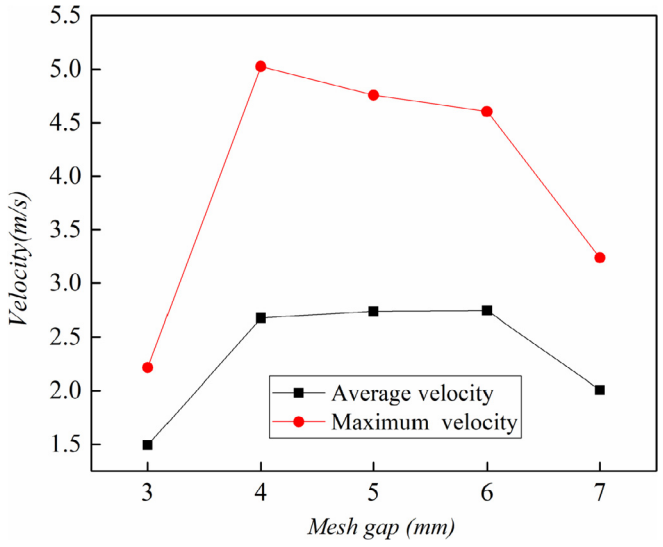

Fig. 12. The velocity characteristics according to mesh gap.

3.3. Effect of the section area of regular hexagon

Section area of regular hexagon is an important configuration factor which determines the size of the ionic wind pump. What's more, it directly influences the characteristics and development of velocity field. In the investigation about section area, the applied voltage, mesh gap, number of needle electrodes and eccentricity are 14 kV, 4 mm, 1 and 0.26 respectively.

As is shown in Fig. 13, both average velocity and maximum velocity decline with the increase of the section area of regular hexagon. The average velocity reaches maximum value, which is 2.67 m/s, and the maximum velocity reaches maximum value, which is 5.03 m/s, when the section area of the regular hexagon is 99.87 mm^2. With the decrease of the section area, the distribution of air jet sources is more concentrative, and the average velocity will increase accordingly. Thus, a smaller section area could get a superior velocity performance in this investigation.

3.4. Effect of the needle electrode number

Obviously, changing the corona electrode number in a single ionic wind unit could greatly affect the performance of the ionic wind pump in velocity characteristics. The distribution of needle electrodes is shown in Fig. 9 when its number is 3 and 6. In the investigation of the needle electrode number, the applied voltage, eccentricity and side length of regular hexagon is set as 14 kV, 0.26 and 9.58 mm respectively.

As is shown in Fig. 14, with the increase of needle electrode

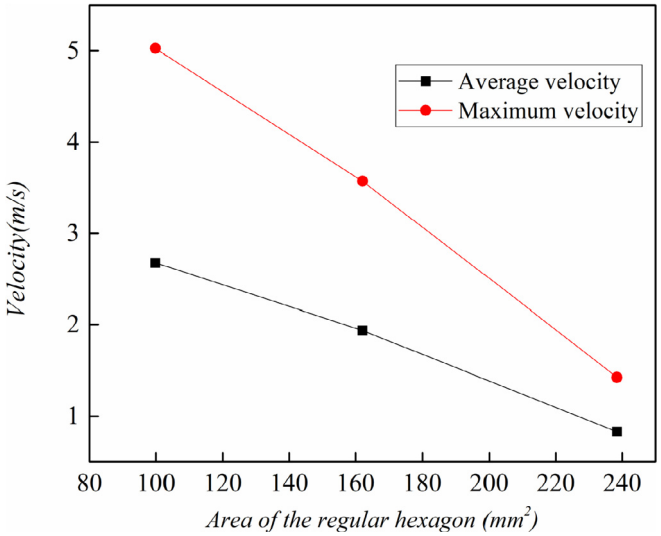

Fig. 13. The velocity characteristics with the section area of 99.87 mm^2, 162.15 mm^2 and 238.44 mm^2, respectively.

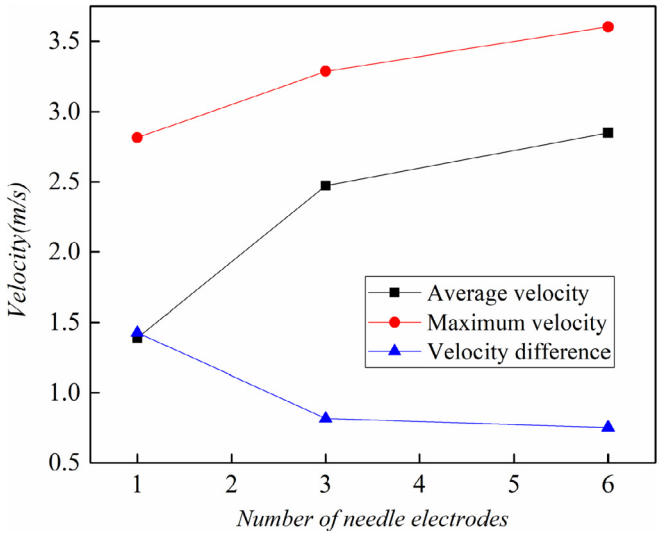

Fig. 14. The velocity characteristics with number of needles (1, 3 and 6, respectively).

number, both average velocity and maximum velocity increase, and the velocity difference between average velocity and maximum velocity declines. When the number of needle electrodes is 6, average velocity and maximum velocity reach their maximum values, which are 2.85 m/s and 3.60 m/s, while the velocity difference reaches minimum value, which is 0.75 m/s. Fig. 15 shows the velocity distributions when needle electrode number is 1, 3 and 6, and the differences between different velocity fields are shown clearly.

With the increase of the needle electrode number, the interaction between different needle electrodes becomes increasingly stronger, and this interaction limits the development of the air flow. Thus, average velocity and maximum velocity increase with the increase of the needle electrode number but not in a multiple relation. However, the interaction could make the flow more uniform because of the momentum exchange. Therefore, the distribution of velocity is more uniform when the number of needle electrodes increases. It could be concluded that increasing the needle electrode number is a feasible approach to enhance the outlet velocity and improve the velocity distribution.

4. Experimental characteristics of the optimized model

After the investigation of every single configuration factor, the optimal configuration factors are selected to develop an optimized integrated ionic wind pump. Then, the experimental investigation of velocity characteristics is carried out to demonstrate the performance of our optimization. In the optimized unit, mesh gap and eccentricity are 6 mm and 0.26, respectively. Considering the limited machining process, 238.44 mm^2 and 3 are chosen as the final section area and the final needle electrode number although the velocity performance is not the best.

Fig. 16 shows the 3-D configuration of the optimized model. Compared to the preliminary model, the needle electrode number is greater and the collector electrode is denser. Fig. 17 shows the effect of voltage on average outlet velocity in preliminary and optimized model. As is shown in this figure, average velocity increases with the increase of applied voltage in both of the models. When the applied voltage is 15 kV, the velocity of preliminary model reaches its maximum value, which is 2.03 m/s, while the optimized model has a higher maximum velocity, which is 2.30 m/s, in the same applied voltage. The corona onset voltage of the

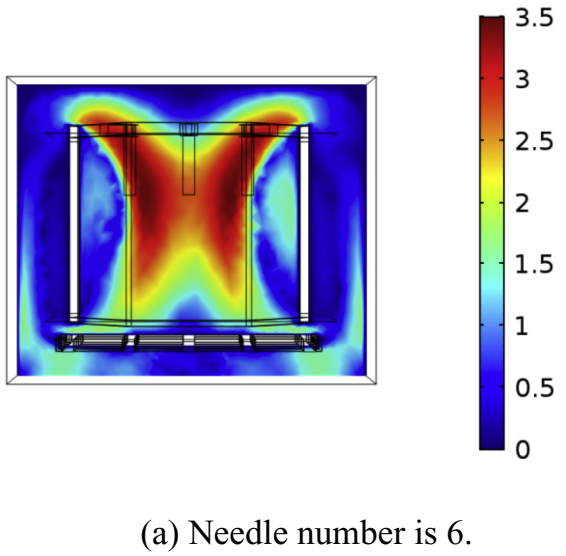

(a) Needle number is 6.

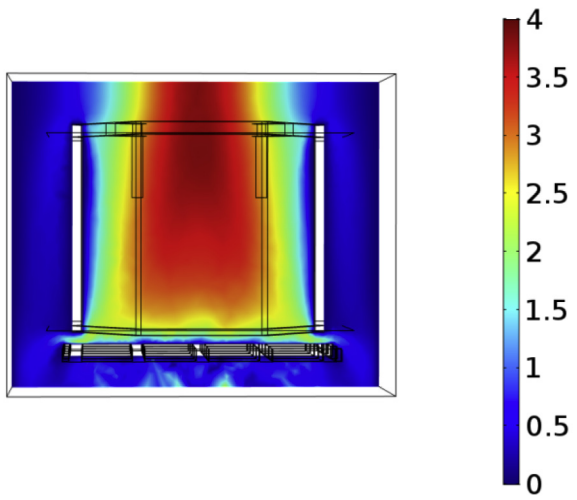

(b) Needle number is 3.

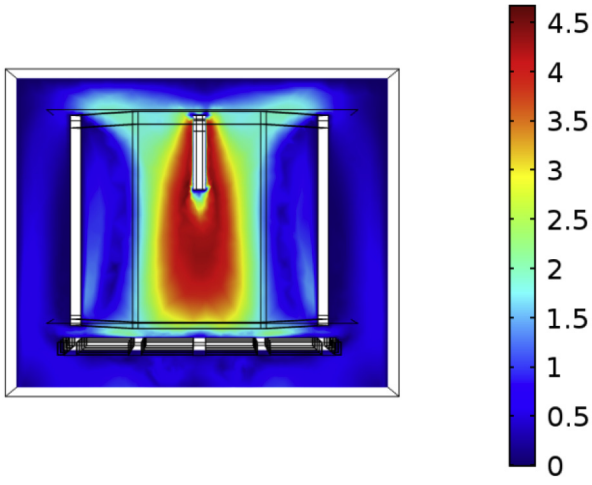

(c) Needle number is 1.

Fig. 15. The velocity distributions.

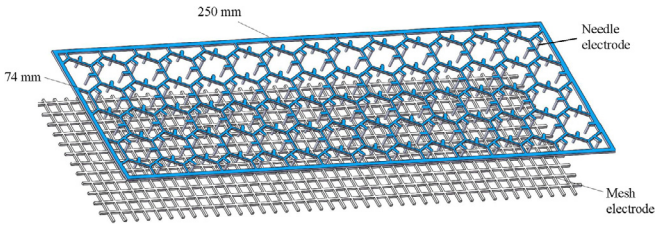

Fig. 16. The 3-D schematic diagram of the optimized model.

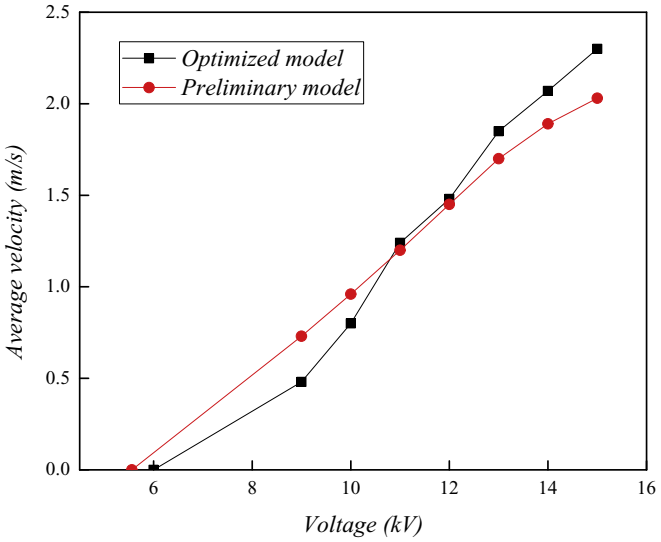

Fig. 17. The velocity characteristic according to voltage.

optimized model, which is 6 kV, is higher than the corona onset voltage of the preliminary model, which is 5.56 kV. Compared with the preliminary model, the optimized model has a sharper increase curve. A possible reason could be that the optimized model has many more needle electrodes than the preliminary model, which means that higher applied voltage is required to start the optimized model. When the applied voltage is higher than the corona onset voltage, ionic wind will be generated and every single needle electrode could be regarded as a minute gas jet source. Thus, more needle electrodes could generate a stronger response to the applied voltage, and the velocity will increase more sharply correspondingly.

5. Conclusions

The experimental and numerical investigations of the large-size ionic wind pump were accomplished to improve the velocity characteristics. The following conclusions have been formulated.

1. The number and the location of needle electrodes affect velocity significantly. Increasing the number of needle electrodes is a feasible approach to enhance the outlet velocity and improve the velocity distribution. The eccentricity of needle electrodes has an optimal value to the ionic wind pump, which is 0.26 in our investigations.
2. Mesh electrode performs better than ring electrode in our investigations. With the increase of mesh gap, flow resistance decreases and energy conversion efficiency increases. There is an optimal value to velocity of 6 mm in our investigations.
3. After the structure optimization, the maximum velocity of 2.30 m/s of the optimized pump is higher than the preliminary model by 13.3%. The maximum volumetric flow reaches 2553 L/min while the power is only 27.59 W.

Acknowledgments

This work was supported by the National Natural Science Foundation of China (No. 51576155) and the Foundation for Innovative Research Groups of the National Natural Science Foundation of China (No. 51721004).

References

[1] Go David B, et al. Ionic winds for locally enhanced cooling. J Appl Phys 2007;102(5):654–1930.
[2] Kim Bumchang, et al. Ion wind generation and the application to cooling. J Electrost 2012;70(5):438–44.
[3] Dong Ho Shin, Yoon JS, Han SK. Experimental optimization of ion wind generator with needle to parallel plates for cooling device. Int J Heat Mass Tran 2015;84:35–45.
[4] Dong Ho Shin, Baek SH, Han SK. Development of heat sink with ionic wind for LED cooling. Int J Heat Mass Tran 2016;93:516–28.
[5] Vatazhin AB, Ulybyshev KE. "Ion wind", a gas-dynamic flow in the corona discharge, and its interaction with the external flow. Fluid Dyn 2012;47(2):206–13.
[6] Colas Dorian F, et al. Ionic wind generation by a wire-cylinder-plate corona discharge in air at atmospheric pressure. J Appl Phys 2012;108(10):103306. 103306-6.
[7] Robinson Myron. Movement of air in the electric wind of the corona discharge. Am Inst Electric Eng Part I Commun Electron Trans 1961;80(2):143–50.
[8] Molki Majid, et al. Heat transfer enhancement of airflow in a channel using corona discharge. J Enhanc Heat Transf 2000;7(6):411–25.
[9] Kalman H, Sher E. Enhancement of heat transfer by means of a corona wind created by a wire electrode and confined wings assembly. Appl Therm Eng 2001;21(3):265–82.
[10] Léger Luc, et al. Influence of a DC corona discharge on the airflow along an inclined flat plate. J Electrost 2001;51(1):300–6.
[11] Chen Ing Youn, et al. Enhanced cooling for LED lighting using ionic wind. Int J Heat Mass Tran 2013;57(1):285–91.
[12] Kim C, et al. Velocity and energy conversion efficiency characteristics of ionic wind generator in a multistage configuration. J Electrost 2010;68(1):36–41.
[13] Ohyama S, Ohyama R. Ionic wind characteristics of an EHD micro gas pump constructed with needle-ring electrode system. Electric Insulat Dielectric Phenom IEEE 2012:227–30.
[14] Wei Qiu, et al. Experimental study on the velocity and efficiency characteristics of a serial staged needle array-mesh type EHD gas pump. Plasma Sci Technol 2011;13(6):693.
[15] Li Longnan, et al. An empirical model for ionic wind generation by a needle-to-cylinder dc corona discharge. J Electrost 2015;73:125–30.
[16] Lee Seung Jun, et al. Parallel integration of ionic wind generators on PCBs for enhancing flow rate. Microsyst Technol 2015;21(7):1465–71.
[17] Rickard Matthew, Dunn-Rankin Derek. Numerical simulation of a tubular ion-driven wind generator. J Electrost 2007;65(10–11):646–54.
[18] Perez AT, et al. Numerical study of an electrohydrodynamic plume between a blade injector and a flat plate. IEEE Trans Dielectr Electr Insul 2009;16(2):448–55.
[19] Zhao Lin, Adamiak Kazimierz. Numerical simulation of the effect of EHD flow on corona discharge in compressed air. IEEE Trans Ind Appl 2013;49(1):298–304.